An Acad Bras Cienc (2022) 94(Suppl. 1): e20210795 DOI 10.1590/0001-3765202220210795
Anais da Academia Brasileira de Ciências | *Annals of the Brazilian Academy of Sciences*
Printed ISSN 0001-3765 I Online ISSN 1678-2690
www.scielo.br/aabc | www.fb.com/aabcjournal

GEOSCIENCES

Response of southern troposphere meridional circulation to historical maxima of Antarctic sea ice

MICHELLY G.S. QUEIROZ, CLÁUDIA K. PARISE, LUCIANO P. PEZZI, CAMILA B. CARPENEDO, FERNANDA C. VASCONCELLOS, ANA LAURA R. TORRES, WESLEY L. BARBOSA & LEONARDO G. LIMA

Abstract: The variability of Antarctic sea ice (ASI) has great potential to affect atmospheric circulation, with impacts that can extend from the surface to the middle and high levels of troposphere. The present study has evaluated the response of South Atlantic tropospheric circulation to increased coverage in area and volume of ASI. Monthly data of air temperature, zonal and meridional wind and mean sea level pressure were obtained from two ensemble simulations performed with the GDFL/CM2.1 model, covering the period from July 2020 to June 2030. In general, the response of South Atlantic tropospheric circulation to increased ASI showed that the climatic signal extended up from the surface to the high levels, propagating as a South Pole–Tropics teleconnection. The results show a general cooling of the southern troposphere, which for instance lead to the strengthening and northward shift of the polar jet and the southward shift of the subtropical jet and to an inversion from the positive to negative phase of the Southern Annular Mode. This study has great relevance for understanding the global climate changes in short term, by assessing the sensitivity of South Atlantic tropospheric circulation to extreme variations in ASI.

Key words: Antarctic Sea Ice, Atmospheric Circulation, South Atlantic Ocean, Hadley Cell, Polar Cell.

INTRODUCTION

The variability of Antarctic sea ice (ASI) is of a great importance for the thermal balance of global climate system, since it affects the dynamics of the southern ocean and atmosphere, with impacts that propagate from the surface to the high levels of troposphere (e.g., Hudson & Hewitson 2001, Raphael et al. 2011, Kidston et al. 2011, Parise 2014, England et al. 2018, Ayres & Screen 2019). As a consequence, expansion and reduction events of ASI end up generating local disturbances that can spread out to remote areas of globe, impacting the tropical climate through teleconnections (Yuan & Martinson 2000, Liu & Alexander 2007). In this context of teleconnections, changes in the tropics can also impact the polar climate (Carleton 2003, Liu & Alexander 2007, Yuan & Li 2008, Yuan et al. 2018). In El Niño events, for instance, sea surface temperature (SST) anomalies in the central-eastern Tropical Pacific increase the air convection in the region, altering the southern meridional thermal gradient (Yuan 2004, Yuan et al. 2018). A planetary waves train spreads from Tropical Pacific towards South America (Pacific-South American mode - PSA) (Mo & Paegle 2001) and acts on the atmospheric patterns of meridional circulation cells and the interannual

variability of ASI, especially in Pacific and Atlantic sectors (Yuan & Martinson 2001, Liu et al. 2002, Carpenedo & Ambrizzi 2016, Cerrone & Fusco 2018).

Even with high seasonal variability, studies have shown an increasing trend in ASI until the year 2014 (e.g., Holland & Kwok 2012, Bintanja et al. 2013, Meehl et al. 2016, Li et al. 2020). From 2014 to 2017, a decreasing trend in ASI was documented, with 2017 presenting the last low record (e.g., Parkinson 2019, Wang et al. 2019, Turner et al. 2020). Although a significant reduction in ASI coverage may also modify the atmospheric circulation, expansion events of ASI have a much greater impact, likely because the sea ice melts faster and freezes more slowly (Carpenedo & Ambrizzi 2016, Carpenedo 2017). Under the scenario of historical increase in ASI, Parise (2014) and Parise et al. (2015) observed a cooling of the air temperature in high and mid-latitudes, an intensification of the polar jet, and the establishment of the positive phase of the Southern Annular Mode (SAM), with impacts varying seasonally and accordingly to the sector (Atlantic, Pacific and Indian Oceans). These authors have shown that the maxima applied to the ASI field have persisted during the first 4 years of model simulation, when eventually the ASI field passes to present the climatological pattern. The disturbance applied to the ASI, however, resulted in cold and fresh melting water, which was able to influence the buoyancy of the Southern Ocean and the surrounding atmosphere, by limiting ocean-atmosphere heat exchanges also during the following 4 years of simulation (Parise et al. 2015).

By examining the influence of ASI distribution on the Southern Hemisphere large-scale circulation based on a fully coupled general circulation model, Hudson & Hewitson (2001) found that minimum ASI conditions in the southern summer caused a strengthening and a poleward shifting of the Hadley circulation. Also, in an ASI reduction scenario, Raphael et al. (2011) showed that there is an expansion of the Polar cell and subsequent displacement of the Ferrel cell towards the equator. In addition to these results, Raphael et al. (2011) pointed out that small changes in surface air temperature can result in large impacts on the southern climate, since the ASI edge is located in the latitudinal zone (approximately 60°S) of high thermal gradients, known as the Polar Front or Antarctic Convergence (Rabelo et al. 2009). Therefore, these ASI changes alter the surface circulation and the deep-water formation, with impacts on the ecosystem and the atmosphere-ocean-ice interactions (Li et al. 2020).

In this way, due to the influence of polar regions on global climate variability and to the most pronounced changes on atmospheric circulation over the twentieth and twenty-first century taking place in the South Atlantic and Pacific sectors (Screen et al. 2018), the present study evaluates the response of the meridional circulation cells, in the South Atlantic sector, to a historical increase in ASI area and volume. In addition, we investigate the time required for the climate signal generated from the ASI disturbances finally reaches the tropical troposphere. The propagation mechanisms of the climate signal from southern high to low-latitudes are also evaluated.

ATMOSPHERIC DATA AND ANALYSES

Monthly air temperature, zonal and meridional wind and mean sea level pressure (MSLP) data simulated by the Coupled Climate Model of the Geophysical Fluid Dynamics Laboratory of the National Oceanic and Atmospheric Administration (GFDL/NOAA), version 2.1 (Model CM2.1) were obtained from the study of Parise (2014), comprising the period from July 2020 to

June 2030 (10 years of simulation). The CM2.1 stands out among the models used for the Fourth Assessment Report of the Intergovernmental Panel on Climate Change (IPCC), published in 2007, for presenting one of the best performances in terms of atmospheric dynamics (e.g., Reichler & Kim 2008). It is composed of four components (oceanic, atmospheric, sea ice and terrestrial) that interact with each other through a flux coupling module, the Flexible Modeling System. More detailed information about each model component is found in Bryan (1969), Semtner (1976), Winton (2000), Delworth et al. (2002), Milly & Shmakin (2002), Gnanadesikan et al. (2006), Stouffer et al. (2006) and Wittenberg et al. (2006). Regarding the sea ice component (Sea Ice Simulator, Winton 2000), the numerical experiments used in this study were conducted with a sophisticated multi-layer model (3 layers, 1 of snow and 2 of ice), that considers thermodynamic and dynamic processes and rheological features of the sea ice.

The climate sensitivity experiments to ASI changes, here named *layer*, had their initial conditions of ASI concentration and thickness perturbed with an expansion extreme field (*layermax* experiment). This was compared to a control experiment initialized from a climatological condition of ASI (*layerctl* experiment). Each experiment was carried out as an ensemble with 30 members each. The initial conditions for the *layerctl* ensemble were generated from restarts files for the months of July, August and September (the two months preceding and the month that presents, climatologically, the largest sea ice cover in the Southern Hemisphere) of a coupled simulation integrated for 10 years (totaling 30 members). The maximum concentration of ASI, in turn, was calculated from the Met Office Hadley Center (HadISST1) data set (1870-2008) (Rayner et al. 2003), while the maximum thickness was calculated from a monthly climatology provided by the GFDL (1979-1996) (Taylor et al. 2000). Both conditions of ASI area and volume were designed to represent the maximum value of sea ice in the whole time series for each grid point, regardless of when it has occurred in time. More details on the sensitivity experiments used in this study are found in Parise (2014) and Parise et al. (2015).

In the present study, the impacts of the increase on ASI in the South Atlantic troposphere are assessed through the *layermax-layerctl* differences of the zonal mean profiles and Hovmöller diagrams (latitude *vs* time) for the lower (850 hPa) and higher (250 hPa) levels. This diagram stands out in showing the movement or displacement of an anomaly through static images, calculating the average of all values in a single line of longitude or latitude (Hovmöller 1949).

In this study, the *y* axis represents the latitudes from 90°S to 30°N, while the *x* axis represents time in years (from July 2020 to June 2030). In order to verify the tropospheric changes between the middle (40°S) and high (65°S) latitudes over the 10 years of the coupled model simulation, we analyzed the *layermax-layerctl* differences for air temperature, zonal and meridional wind at 850 hPa and 250 hPa levels and MSLP. The MSLP differences between middle and high latitudes were calculated based on the methodology proposed of Marshall (2003).

To verify the response timing of vertical structure of the South Atlantic troposphere in view of expansion extremes imposed on the ASI concentration and thickness, the zonal mean profiles were calculated separately for three specific periods. These periods were predetermined as a function of the Southern Ocean memory to the initial condition of ASI (Parise et al. 2015), based on its distinct phases: when de *layermax-layerctl* differences were

positive (July 2020 – June 2024), close to zero (July 2024 – June 2028) and negative (July 2028 – June 2030), respectively, in relation to the ASI maxima (Parise 2014, Parise et al. 2015). In this way, the study sought to evaluate the behavior of climate response on an interannual timescale, aiming to discuss the possible consequences for the South America climate. The domain of the southern troposphere analyzed here comprises the latitudes from 90°S to 30°N and longitudes from 65°W to 15°E (Atlantic sector).

RESULTS

Response of South Atlantic meridional circulation to Antarctic sea ice maxima

From this section onwards, we started to show the results from our study obtained through numerical modeling experiments, when ASI extremes were imposed as initial conditions for each ensemble member. The differences of ASI concentration (%) and thickness (m) between the *layermax-layerctl* ensemble experiment averages in the Atlantic sector (60°W – 20°E) for the 10 years of model simulation (2020 – 2030) are shown in Figure 1. The results show that the ASI in Atlantic sector was larger than climatological pattern during the first 7 years of simulation, when it has passed to a negative phase of ASI. Parise et al. (2015), by analyzing the climate memory to ASI changes, have found a period of 4 years for the whole perturbance applied to ASI completely melts and more 4 years for the cold and fresh surface melting water be transported from Southern Ocean to the Tropical Ocean. The interannual variability of the Weddell Sea ice has large influence on the atmospheric circulation over the South Atlantic sector (Morioka et al. 2017). Furthermore, accurate initialization of sea ice conditions during southern winter is a key element for a skillful prediction of climate variability over the Weddell Sea during the next

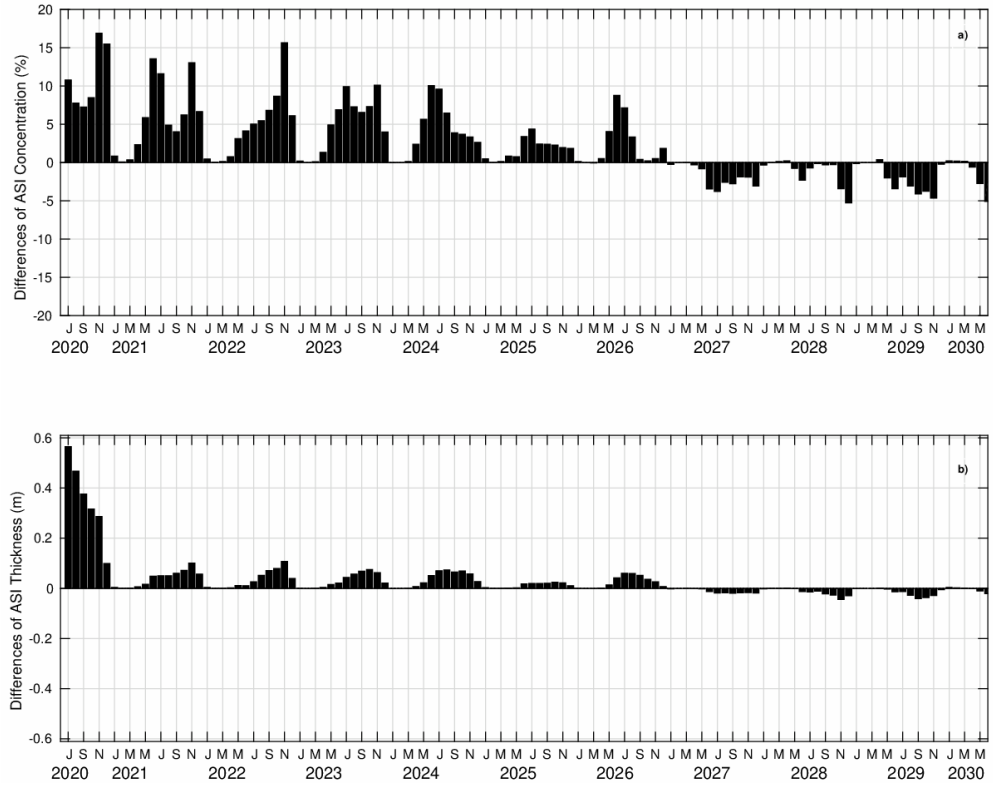

Figure 1. Differences of Antarctic sea ice (ASI) a) concentration (%) and b) thickness (m) between the *layermax-layerctl* ensemble experiments in Atlantic sector (60°W–20°E) for the 10 years of model simulation (July 2020–June 2030).

season, i.e., in southern spring (Morioka et al. 2019).

The vertical structure of the air temperature in the Atlantic sector is shown in Figure 2. The results show a general cooling of the southern troposphere (down to -0.6°C) from the surface to the high levels (approximately 300 hPa), especially between the high and mid-latitudes (90°S and 45°S) from 2020-2024 (Figure 2a). The cooling in the mid and high-latitudes of the South Atlantic suggest an increase in the meridional thermal gradients, until 8 years following expansion extreme of ASI (Figures 2a and 2b). Also, a small surface cooling (approximately 0.2°C) is found over the equatorial region (from 5°S to 5°N) during the first 8 years of model simulation (Figures 2a and 2b). During this period, the impacts on the tropical region have concentrated at the upper levels. In the last 2 years of simulation (2028-2030), this tropospheric cooling has spread out over the tropics, from the surface and more strongly at high levels (Figure 2c). Between 75°S to 55°S, we observed a maximum cooling of -0.6°C in the period from July 2020 to June 2024. On the other hand, a slight warming of ~+0.2ºC is found from the surface to the mid-levels of troposphere five years later, in the period from July 2028 to June 2030. By analyzing the atmospheric response to ASI loss, England et al. (2018) have found a confined latitudinally (over the high-latitudes) and vertically (up to 600 hPa) warming at the high levels of troposphere. Even though the present study is analyzing the impacts of an ASI increase, it is important to understand that, since the experiments were conducted with a coupled model without any flux or variable adjustments, there is a progressive loss of sea ice as the CM2.1 model runs. Due to the presence of sea ice normally acts on decreasing the surface air temperature, and vice-versa, this thermodynamic response was already expected. Therefore, in the present study we found the air temperature biases can generate anomalies that reach the upper-levels of troposphere. These results corroborate with Raphael (2011), Parise (2014), Parise et al. (2015) and Carpenedo & Ambrizzi (2016), who also found a cooling of the atmosphere in an extremely positive ASI condition. Parise (2014) and Parise et al. (2015) showed that this colder air mass was displaced towards the lower latitudes (from Antarctic

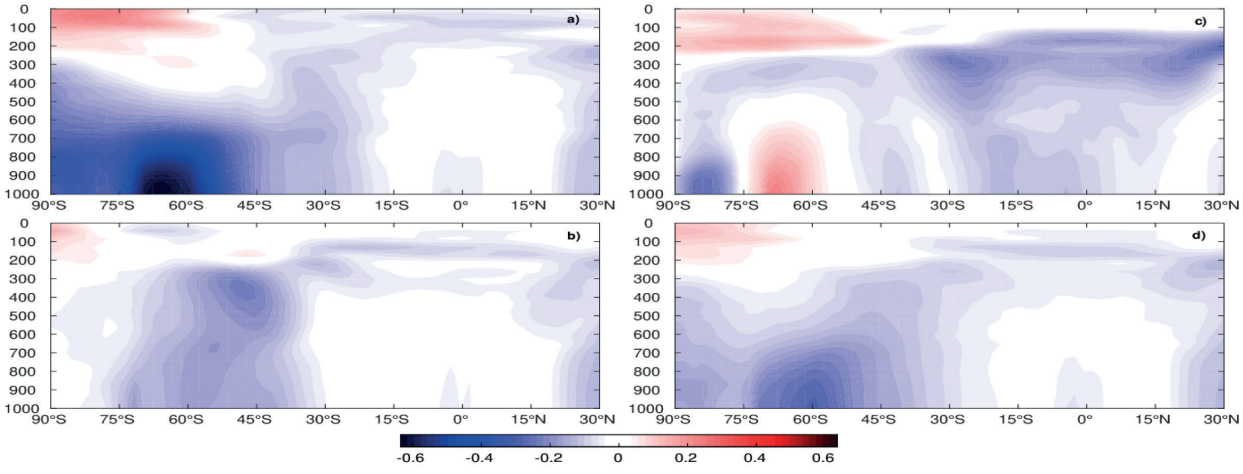

Figure 2. Differences between the *layermax-layerctl* experiments for the zonal mean (from 90°S to 30°N) air temperature profile (°C) for the Atlantic sector (from 65°W to 15°E) during the periods: a) July 2020–June 2024; b) July 2024–June 2028; c) July 2028–June 2030 and d) July 2020–June 2030.

to Equator) in its greatest amount during the southern spring (SON), precisely in the season of the ASI climatological maximum (Parkinson 2019). When ASI is at its extreme maximum, there is an increase in albedo and a consequent reduction in absorption of shortwave radiation. With less energy being absorbed by the surface, a reduction occurs in both SST and vertical heat fluxes, especially over the ASI edge. Morioka et al. (2017) found that the reduction of sea ice in the Weddell Sea sector contributes to the anomalous warming of the surface temperature in the range of 60-70°S and, as a consequence, there is an increase in stability in the atmospheric boundary layer to the north of this strip, implying favorable conditions for the support of anticyclonic anomalies in the lower troposphere in the South Atlantic.

The vertical structure of the zonal mean wind in the Atlantic sector is shown in Figure 3. In the tropical region, the ASI sensitivity experiments showed the intensification of the Hadley cell, with trade winds more intense (easterlies, with negative sign). This intensification took place initially in the Northern Hemisphere (for the periods of 2020–2024 and 2025–2028) and later established itself in both hemispheres. The results also showed the strengthening of the Polar cell in the *layermax* in relation to the control experiment (westerlies between 50°S and the South Pole, with positive sign) and the southward expansion of the Ferrel cell (easterlies between 30ºS and 50°S, with negative sign) (Figure 3a). The disturbance applied on the surface was able to generate a climatic signal that extended up to the high levels of the tropical troposphere, propagating from Antarctica to Tropics. During the first 4 years of model simulation, there was a northward shift of the polar jet and a southward shift of the subtropical jet (Figure 3a). In the following 4 years (2025-2028) there was a southward shift of the atmospheric meridional circulation cells in the South Atlantic sector, with the subtropical jet acting at 35°S and the polar jet at 55°S, approximately (Figure 3b). This response pattern has intensified the wind shear at mid-latitudes (~ 44°S) (Figure 3b). For the period from July 2028 to June 2030, breaks in the vertical structure of the climate oscillations generated in Antarctica were observed, resulting in a smaller wave number (Figure 3c). In the studies of Parise (2014) and Parise et al. (2015)

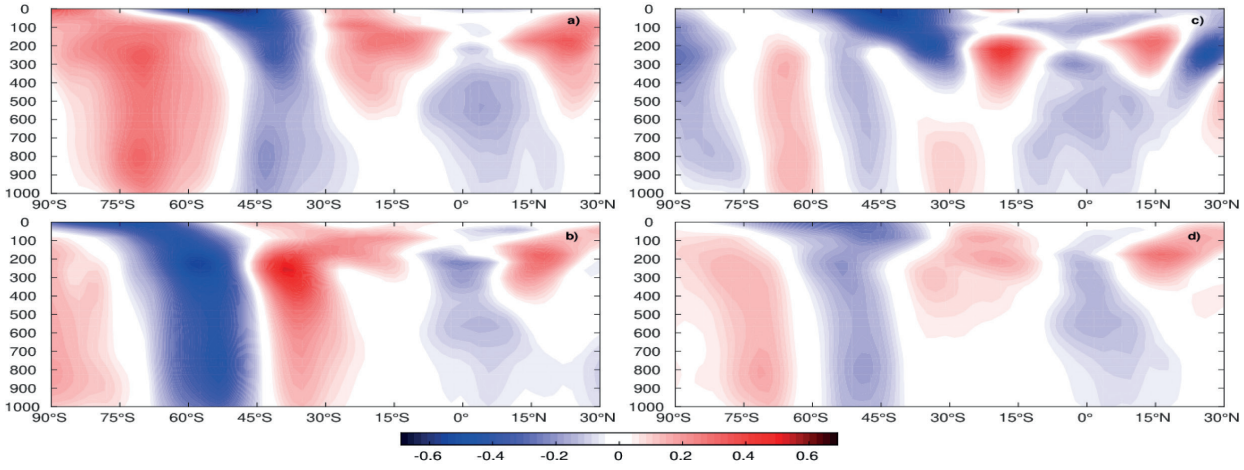

Figure 3. Differences between the *layermax-layerctl* experiments for the zonal mean (from 90°S to 30°N) wind profile (ms^{-1}) for the Atlantic sector (from 65°W to 15°E) during the periods: a) July 2020–June 2024; b) July 2024–June 2028; c) July 2028–June 2030 and d) July 2020–June 2030.

positive zonal wind anomalies were found at 50°S in the southern spring (SON), between 55°S and 75°S in the autumn (MAM) and south of 65°S in the winter (JJA), being stronger in the last. By analyzing maximum conditions of ASI for southern summer, Raphael (2003) found that the entire southern circulation cell seems to move northwards, with the mid-latitude surface westerly winds becoming weaker and the polar easterlies expanding further north. Also, in response to increased extend of ASI, Kidston et al. (2011) and Smith et al. (2017) observed a poleward shift of the mid-latitude jet stream, as also found in the present study.

When analyzing the climate response to the variability of the radiative (solar) forcing, Haigh et al. (2005) suggest that the expected dynamics of the troposphere is due in particular to the warming of the stratosphere, with impacts more easily detected in the subtropical and middle latitudes. This warming tends to weaken the subtropical jets and the southern tropospheric mean circulation, with a weakening and expansion of Hadley cells and a poleward shift of the Ferrel cells. In this way, the positions of the subtropical jets and the extension of Hadley cells respond to the distribution of the stratospheric warming, with the low-latitude warming forcing them to move towards the poles, and high-latitude warming forcing them to move towards the equator (Haigh et al. 2005). Kodera et al. (2016) studying the stratospheric warming events and their influence on the troposphere circulation have reported that the tropospheric connection is more directly related to the vertical structure of planetary waves than the horizontal structure of the polar vortex. The Hadley cell edge is also closely related to temperature gradients occurring over the tropical upper troposphere (Son et al. 2018). By addressing the influence of Atlantic Meridional Overturning Circulation (AMOC) on the position asymmetry of the Intertropical Convergence Zone (ITCZ), which is found slightly north of the equator, Aimola & Moura (2016) have found that anomalous Hadley cell transports particularly moisture at low levels from equator to the Northern Hemisphere and energy at high levels to the Southern Hemisphere, so that the maximum precipitation occurs to the north of equator following the ITCZ position.

The zonal mean profile of meridional wind between 90°S and 30°N is shown in Figure 4. In the period from July 2020 to June 2024

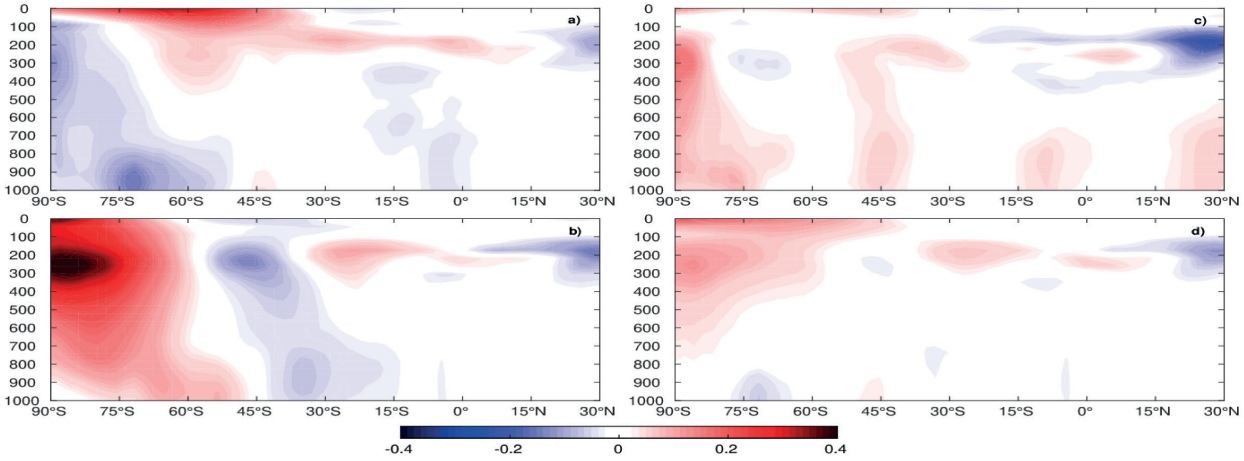

Figure 4. Differences between the *layermax-layerctl* experiments for the meridional mean (from 90°S to 30°N) wind profile (ms^{-1}) for the Atlantic sector (from 65°W to 15°E) during the periods: a) July 2020–June 2024; b) July 2024–June 2028; c) July 2028–June 2030 and d) July 2020–June 2030.

(Figure 4a) we observe negative anomalies of meridional wind between 90°S (almost the entire troposphere) and approximately 50°S (low levels). This anomalous pattern indicates a strengthening of the upper branch of the Polar cell and a weakening of the lower branch, as well as a strengthening of the lower branch of the Ferrel cell. This weakening (strengthening) of the lower branch of Polar (Ferrel) cell may indicate its contraction, which is associated with the expansion extreme of ASI. The same pattern was also observed by Raphael et al. (2011) for the months from January to March. In relation to the tropical circulation cell, a strengthening (weakening) of the upper branch of Hadley cell between ~30°S to 0° (at approximately 30°N), respectively, was verified (Figure 4a).

On the other hand, in the period from July 2024 to June 2028 (Figure 4b), when the maximum ASI has already been melted, there was an inversion of the anomalies observed in the previous period (2020–2024), with a predominance of positive anomalies south of 45°S. The results showed a weakening of the lower branch of Ferrel cell, between approximately 65°S and 45°S, and a strengthening (weakening) of the lower (upper) branch of Polar cell, respectively, with the largest meridional wind anomalies at high levels. Between the middle and low-latitudes there was a predominance of negative anomalies, indicating a strengthening of the lower branch of Ferrel cell between 45°S and 35°S, approximately, and a weakening at high levels. The strengthening of the lower branch of Polar cell may indicate its expansion. One consequence of this strengthening is the displacement of Ferrel cell to the north. This expansion of the Polar cell and consequently the displacement of the middle latitude cell towards the equator was also observed by Raphael et al. (2011) under minimum conditions of ASI in the southern summer. With the Antarctic Polar Front displaced to the north, coinciding with the spatial pattern similar to the negative phase of SAM (see forward in Figure 5b), there is a favor in the propagation of transient systems in southern Brazil, since the subtropical jet is strengthened and displaced towards the equator (Carvalho et al. 2005, Rudeva & Simmonds 2015). Regarding the Hadley cell, a pattern similar to first period analyzed (2020–2024) is observed for its upper branch even if a weakening at approximately 30°S to 15°S is observed for its lower branch (Figure 4b).

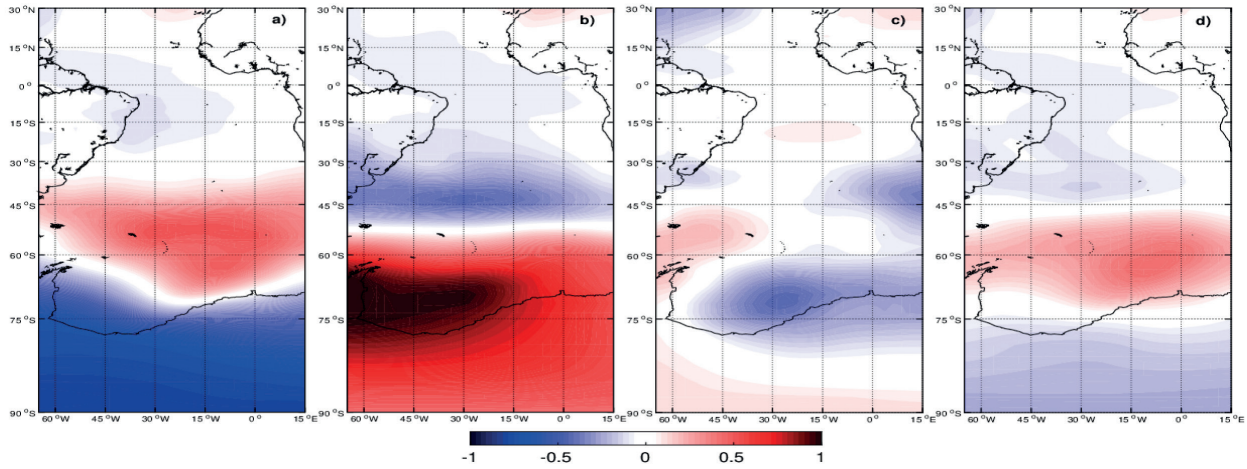

Figure 5. Differences between *layermax-layerctl* experiments for mean sea level pressure (hPa) during the periods: a) July 2020–June 2024; b) July 2024–June 2028; c) July 2028–June 2030 and d) July 2020–June 2030.

Finally, in the period from July 2029 to June 2030 (Figure 4c), the strengthening (weakening) of the lower (upper) branch of Polar cell are observed south of 60°S, while around 45°S there are positive anomalies of meridional wind in practically the entire troposphere, indicating a weakening (strengthening) of the lower (upper) branch of Ferrel cell. In relation to the Hadley cell, we found a strengthening of its upper branch around 30°S and a weakening (strengthening) of its upper (lower) branch at approximately 30°N.

When analyzing the entire simulation period, from July 2020 to June 2030 (Figure 4d), we observed the predominance of positive anomalies of meridional wind at middle and high levels of high southern latitudes, while at low levels there were no biases. Thus, the results show that the largest anomalies were observed especially at high levels of the troposphere in the sector of Polar and Ferrel cells when evaluating the first two simulation periods, indicating that the ASI concentration and thickness changes have a great influence on the displacement and intensity of these tropospheric meridional cells.

The differences of MSLP in the Atlantic sector of Southern Ocean are shown in Figure 5. Positive (negative) differences were observed out of phase between middle- and high-latitudes, indicating an increase (decrease) in the MSLP, respectively. When analyzing the response of the Southern Hemisphere's climate in the three predetermined periods, it was found a spatial pattern similar to the positive (2020–2024) and negative (2024–2028) phase of the SAM (Thompson & Wallace 2000, Gillett et al. 2006).

The positive (negative) anomalies of MSLP found over the subtropical zone during 2020–2024 (2025–2028) periods suggests a slight strengthening (weakening) of the South Atlantic Subtropical High (SASH) (Figures 5a and 5b). For the 2020–2024 period, this positive bias of MSLP found in mid-latitudes does not reach the tropical region, where negative biases are observed. From July 2024 to June 2028, the MSLP anomalies are in association with the weakening of the Hadley cell in the Southern Hemisphere (positive anomalies of zonal wind at middle and high levels) (Figure 3b). Considering the temporal average of the entire simulation period of the coupled model, higher (lower) MSLP were found in the middle (high) latitudes, respectively (Figure 5d), which is consistent with the positive phase of SAM, as also shown in Raphael et al. (2011) and Parise et al. (2015). In the studies by Parise (2014) and Parise et al. (2015) it was found that considering the entire simulation period (2020–2030) there was a decrease in MSLP in high-latitudes (~ 3 hPa) and an increase in mid-latitudes (~ 1.5 hPa), being the response of this field most significative in southern autumn (MAM) and winter (JJA). According to Pezza et al. (2012), in La Niña years occurring with a positive phase of SAM would present the most favorable conditions for the general growth of sea ice (except to the west of Antarctic Peninsula, where the opposite is seen). Any trend in SAM can have highly significant impacts on regional precipitation patterns (Gupta & England 2006). In the positive phase of SAM (i.e., positive anomalies of MSLP in mid-latitudes), SASH tends to be positioned further south (Sun et al. 2017, Carpenedo & Ambrizzi 2020), influencing the strengthening of trade winds in some areas at south of northeast region of Brazil (Carpenedo & Ambrizzi 2020). Oppositely, in the negative phase of SAM, the SASH tends to be positioned further north, generating negative anomalies of precipitation in the north and northeast regions (Carpenedo & Ambrizzi 2020).

Regarding the *layermax-layerctl* differences for air temperature (250 hPa and 850 hPa), zonal wind (250 hPa and 850 hPa) and MSLP between

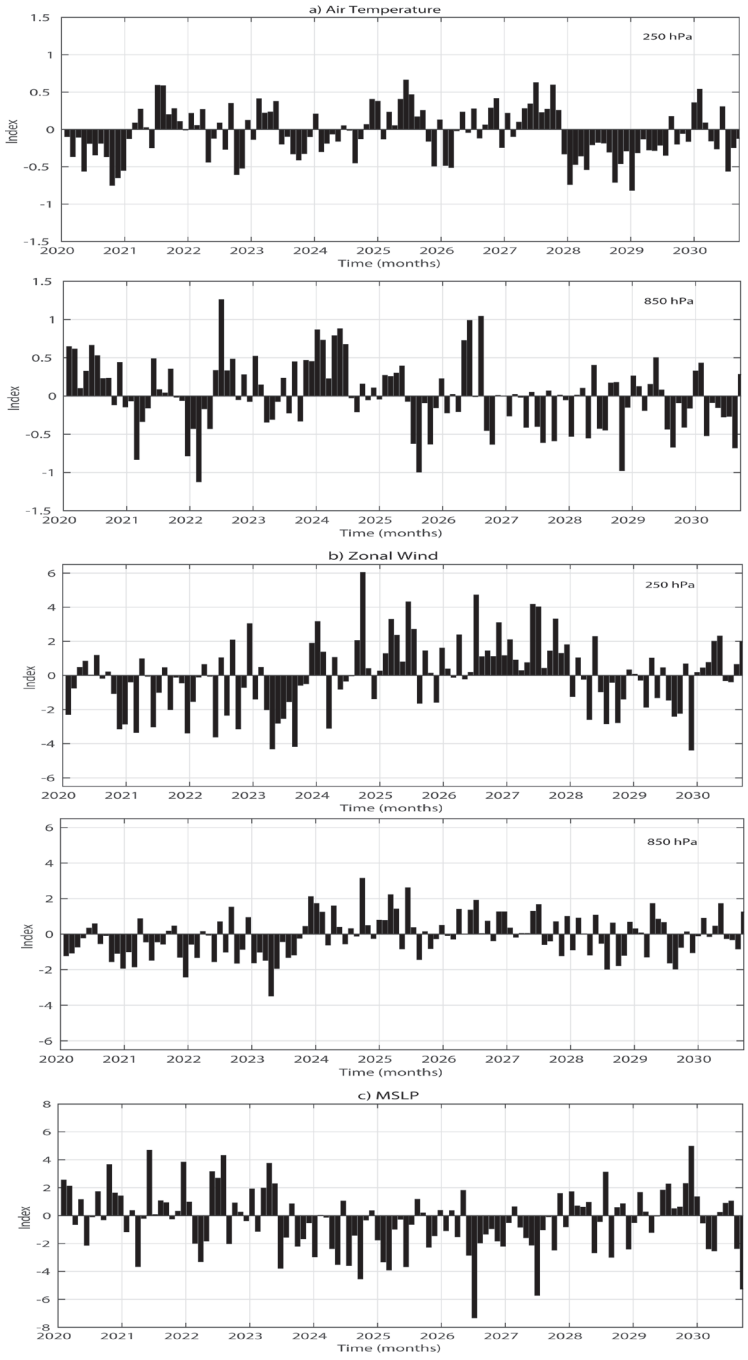

Figure 6. Differences between *layermax-layerctl* experiments at middle (40°S) and high (65°S) latitudes for: a) 250 hPa and 850 hPa air temperature; b) 250 hPa and 850 hPa zonal mean wind and c) MSLP during the whole period of CM2.1 model simulation (2020–2030).

the 40°S and 65°S latitudes, it was found that for air temperature (Figure 6a) the positive and negative differences were higher at low levels (850 hPa), reaching up to ~1.3°C in the first 4 years of simulation (2020–2024). In relation to the zonal wind (Figure 6b) it was observed that the positive and negative differences were greater at high levels (250 hPa) with more positive differences in the period from July 2024 to June 2028, up to approximately 6 ms^{-1}. Finally, the MSLP (Figure 6c) showed more positive differences in the first 4 years of simulation compared to the following 4 years (2025–2028)

where more negative differences were observed, up to approximately -7.8 hPa.

When analyzing the Hovmöller diagrams, it was found that the differences of atmospheric fields are greater. The air temperature (Figure S1 – Supplementary Material), showed throughout the analyzed period (2020–2030) a heating of up to ~1.5°C at the upper troposphere, especially from 90°S to 45°S (Figure S1a). On the other hand, at low levels (Figure S1b) we observed a cooling of up to ~-1.5°C, with emphasis on the first 4 years of simulation (2020–2024).

Regarding the zonal wind (Figure S2), it was observed that the biggest changes occurred at the high levels of troposphere, with an intensification of winds up to 3.5 ms^{-1} in high and middle latitudes (from 90°S to 45°S) for the first 4 years of simulation (2020–2024). In the first 4 years of simulation (2020–2024), the MSLP showed a predominance of negative differences in the high-latitudes and positive differences in the mid-latitudes (up to ~8.0 hPa) (Figure S3). The opposite pattern was observed in the following 4 years (2025–2028).

Regarding climate teleconnections, Cabré et al. (2017) found that changes in deep ocean convection have large and rapid implications for both the extratropics and tropics, causing significant changes in atmospheric temperatures, westerly wind speeds, Hadley circulation, as well as in the inter-hemispheric thermal gradients, atmospheric transport of energy and the position of ITCZ. Bowman & Carrie (2002) showed that there is a semipermeable barrier for transporting properties between the tropics and extratropics. According to them, the atmosphere can be divided into three main parts, the extratropics of Southern Hemisphere, the tropics and the extratropics of Northern Hemisphere. Climatologically, the dispersion of particles within each part of the atmosphere is fast, while the exchange between the different parts is very slower. The entrainment of extratropical air into the tropics in the boundary layer must be matched in the long run by transporting air from the tropics back to the extratropics through the transport barrier (Bowman & Carrie 2002). Liu & Alexander (2007) concluded that the tropical impact on the extratropical climate occurs mainly through the atmosphere, while changes in the extratropics can also impact the tropical climate through the subtropical cells of the upper ocean in decadal and longer time scales. Raphael (2003) and Raphael et al. (2011) also showed that the southern atmosphere is sensitive to extreme ASI scenarios from the surface to the upper-levels, with the largest impacts occurring at middle and low-latitudes. The inversion between the phases of SAM associated to changes in air temperature, winds and MSLP found in our study have a great influence on climate variability in the South Atlantic sector, with impacts on the occurrence of cold fronts in South America, as discussed in the studies performed by Parise (2014) and Caldas et al. (2020). Although a decrease in the ASI has been observed in recent years, with a large impact also on global climate variability, the present study has showed that the ASI increase has the potential to significantly affect the atmospheric circulation in short term. However, a better assessment of the long-term ice-ocean-atmosphere relationship is important to understand the impacts of this scenario.

CONCLUSIONS

The present study sought to evaluate the response of the southern meridional atmospheric circulation cells in the Atlantic sector of the Southern Ocean under a historical maximum condition of ASI, with the focus on the changes occurred in air temperature, zonal and meridional wind and MSLP. For all the ASI

anomalies analyzed (positive, close to zero and negative phases), the results have showed a general cooling of the southern troposphere, from the surface to the upper-levels, which led, for instance, to a strengthening and northward shift of the polar jet, a southward shift of the subtropical jet and an inversion from the positive to negative phase of SAM between the positive and close to zero ASI phases. As Parise et al. (2015) have evaluated the SAM based on the average for the whole simulation period (10 years), this inversion on the SAM phase had not yet been shown.

Regarding the *layermax-layerctl* differences between the latitudes of 40°S and 65°S, it was verified that for the air temperature the positive and negative differences were larger at low levels, while for the zonal wind they were larger at high levels. The MSLP presented more positive differences in the first 4 years of simulation compared to the following 4 years (2025–2028), where more negative differences were observed.

In general, the response of the South Atlantic tropospheric circulation to increased ASI showed that the climatic signal extended up from the surface to the high levels, propagating as a South Pole–Tropics teleconnection. Our results showed that the largest anomalies in the meridional circulation cells occurred especially at high levels of troposphere for Polar and Ferrel cells during the first two periods of simulation, from July 2020 to June 2028. In relation to the Hadley cell, we found a strengthening (weakening) of its upper branch between 30°S to 0° (at approximately 30°N). In the Southern Hemisphere, a strengthening of the Polar and Ferrel cells further south of their climatological positions has occurred, as a mechanism for transferring thermal energy to Antarctica to balance the cold bias observed on the surface of Southern Ocean. This surface cooling was resulted from the ASI anomalies applied and by the melting fresh and cold water.

Our study showed a response mechanism of atmospheric circulation cells in the Atlantic sector to the ASI positive extremes, indicating that the ASI concentration and thickness changes have a great influence on the displacement and intensity of these tropospheric meridional cells. The response of the southern troposphere to the ASI positive extremes reported here showed that the disturbance applied on the surface was able to generate a climatic oscillation that extended up to the upper-levels of troposphere, propagating as a Pole–Tropics teleconnection. Although the results found are relevant in the context of global climate changes related to ASI changes, a more detailed assessment of the climate mechanisms acting on the propagation of the climate oscillation from Antarctica to the lower latitudes of the Atlantic sector will be given in a future paper.

Acknowledgments

The authors would like to thank the funding support of Coordenação de Aperfeiçoamento de Pessoal de Nível Superior (CAPES) to the Projects “Advanced Studies in Oceanography of Medium and High Latitudes” (Process 23038.004304/2014-28) and “Use and Development of the Brazilian Earth System Model for the Study of the Ocean-Atmosphere-Cryosphere System in High and Medium Latitudes - BESM/SOAC” (Process 145668/2017-00) and to the funding support of Conselho Nacional de Desenvolvimento Científico e Tecnológico (CNPq) to the Projects “Impactos do Aumento do Gelo Marinho da Antártica no Clima da América do Sul: Simulações por Conjunto x Reanálises” (Process 420406/2016-6) and “Antarctic Modeling Observation System – ATMOS” (Process 443013/2018-7). This publication was also supported by Fundação de Amparo à Pesquisa e ao Desenvolvimento Científico e Tecnológico do Maranhão (FAPEMA) (Process 00850/17). CNPq funds L. P. Pezzi through fellowship of the Research Productivity Program (Process 304009/2016-4). The authors also acknowledge the GFDL Coupled Climate Model Development Team for providing a public version of the model and for all technical support.

REFERENCES

AIMOLA L & MOURA M. 2016. A Influência da Circulação de Revolvimento Meridional do Atlântico na Definição da Posição Média da ZCIT ao Norte do Equador. Uma Revisão. Rev Bras Meteorol 31(4): 555-563.

AYRES HC & SCREEN JA. 2019. Multimodel Analysis of the Atmospheric Response to Antarctic Sea Ice Loss at Quadrupled CO_2. Geophys Res Lett 46(16): 9861-9869.

BINTANJA R, OLDENBORGH GJV, DRIJFHOUT SS, WOUTERS B & KATSMAN CA. 2013. Important role for ocean warming and increased ice-shelf melt in Antarctic sea-ice expansion. Nat Geosci 6(5): 376-379.

BOWMAN KP & CARRIE GD. 2002. The Mean Meridional Transport Circulation of the Troposphere in an Idealized GCM. J Atmos Sci 59(9): 1502-1514.

BRYAN K. 1969. Climate and the ocean circulation: III. The ocean model. Mon Wea Rev 97(11): 806-827.

CABRÉ A, MARINOV I & GNANADESIKAN A. 2017. Global Atmospheric Teleconnections and Multidecadal Climate Oscillations Driven by Southern Ocean Convection. J Clim 30(20): 8107-8126.

CALDAS CF, VASCONCELLOS FC, CAVALCANTI IFA, CARVALHO NO & LOPES IR. 2020. Impact of Antarctic Sea Ice, ENOS, and Southern Annular Mode on Cold Fronts in South America. Anu Inst Geocienc 43(4): 229-237.

CARLETON AM. 2003. Atmospheric teleconnections involving the Southern Ocean. J Geophys Res 108(C4): 8080.

CARPENEDO CB. 2017. Atmospheric blockings associated with the extreme variability of Antarctic sea ice and impacts over South America. Ph.D. thesis, Astronomy, Geophysics and Atmospheric Sciences Institute, University of São Paulo, 237 p.

CARPENEDO CB & AMBRIZZI T. 2016. Células de Circulação Meridional Durante os Eventos Extremos de Gelo Marinho Antártico. Rev Bras Meteorol 31(3): 251-261.

CARPENEDO CB & AMBRIZZI T. 2020. Anticiclone Subtropical do Atlântico Sul Associado ao Modo Anular Sul e Impactos Climáticos no Brasil. Rev Bras Meteorol 35(4): 605-613.

CARVALHO LMV, JONES C & AMBRIZZI T. 2005. Opposite phases of the Antarctic Oscillation and relationships with intraseasonal to interannual activity in the tropics during the austral summer. J Clim 18(5): 702-718.

CERRONE D & FUSCO G. 2018. Low-frequency climate modes and Antarctic sea ice variations, 1982-2013. J Clim 31(1): 147-175.

DELWORTH T, STOUFFER R, DIXON K, SPELMAN M, KNUTSON T, BROCCOLI A, KUSHNER P & WETHERALD R. 2002. Review of simulations of climate variability and change with the GFDL R30 coupled climate model. Clim Dyn 19: 555-574.

ENGLAND M, POLVANI L & SUN L. 2018. Contrasting the Antarctic and Arctic atmospheric responses to projected sea ice loss in the late twenty first century. J Clim 31(16): 6353-6370.

GILLETT NP, KELL TD & JONES PD. 2006. Regional climate impacts of the Southern Annular Mode. Geophys Res Lett 33(23): 1-4.

GNANADESIKAN A ET AL. 2006. GFDL's CM2 Global Coupled Climate Models. Part II: The Baseline Ocean Simulation. J Clim 19(5): 675-697.

GUPTA AS & ENGLAND MH. 2006. Coupled Ocean–Atmosphere–Ice Response to Variations in the Southern Annular Mode. J Clim 19(18): 4457-4486.

HAIGH J, BLACKBURN M & DAY R. 2005. The Response of Tropospheric Circulation to Perturbations in Lower Stratospheric Temperature. J Clim 18(17): 3672-3685.

HOLLAND PR & KWOK R. 2012. Wind-driven trends in Antarctic sea-ice drift. Nat Geosci 5: 872-875.

HOVMÖLLER E. 1949. The Trough-and-Ridge diagram. Tellus 1: 62-66.

HUDSON DA & HEWITSON BC. 2001. The atmospheric response to a reduction in summer Antarctic sea-ice extent. Clim Res 16(2): 79-99.

KIDSTON J, TASCHETTO AS, THOMPSON DWJ & ENGLAND MH. 2011. The influence of Southern Hemisphere sea-ice extent on the latitude of the mid-latitude jet stream. Geophys Res Lett 38: L15804.

KODERA K, MUKOUGAWA H, MAURY P, UEDA M & CLAUD C. 2016. Absorbing and reflecting sudden stratospheric warming events and their relationship with tropospheric circulation. J Geophys Res Atmos 121(1): 80-94.

LI S, CAI W & WU L. 2020. Attenuated Interannual Variability of Austral Winter Antarctic Sea Ice Over Recent Decades. Geophys Res Lett 47(22): e2020GL090590.

LIU J, YUAN X, RIND D & MARTINSON DG. 2002. Mechanism study of the ENSO and southern high latitude climate teleconnections. Geophys Res Lett 29(14): 1679. doi:10.1029/2002GL015143.

LIU Z & ALEXANDER M. 2007. Atmospheric bridge, oceanic tunnel, and global climatic teleconnections. Rev Geophys 45(2): RG2005.

MARSHALL GJ. 2003. Trends in the Southern Annular Mode from Observations and Reanalyses. J Clim 16(24): 4134-4143.

MEEHL GA, ARBLASTER JM, BITZ CM, CHUNG CTY & TENG H. 2016. Antarctic sea-ice expansion between 2000 and 2014 driven by tropical Pacific decadal climate variability. Nat Geosci 9: 590-595.

MILLY PCD & SHMAKIN AB. 2002. Global Modeling of Land Water and Energy Balances. Part I: The Land Dynamics (LaD) Model. J Hydrometeorol 3(3): 283-299.

MO KC & PAEGLE JN. 2001. The Pacific–South American modes and their downstream effects. Int J Climatol 21(10): 1211-1229.

MORIOKA Y, DOI T, IOVINO D, MASINA S & BEHERA SK. 2019. Role of Sea-Ice Initialization in Climate Predictability over the Weddell Sea. Sci Rep 9: 2457.

MORIOKA Y, ENGELBRECHT F & BEHERA SK. 2017. Role of Weddell Sea ice in South Atlantic Atmospheric Variability. Clim Res 74: 171-184.

PARISE CK. 2014. Sensitivity and memory of the current mean climate to increased Antarctic sea ice: The role of sea ice dynamics. Ph.D. thesis, National Institute for Space Research (INPE), 218 p.

PARISE CK, PEZZI LP, HODGES KI & JUSTINO F. 2015. The Influence of Sea Ice Dynamics on the Climate Sensitivity and Memory to Increased Antarctic Sea Ice. J Clim 28(24): 9642-9668.

PARKINSON CL. 2019. A 40-y record reveals gradual Antarctic sea ice increases followed by decreases at rates far exceeding the rates seen in the Arctic. Proc Natl Acad Sci USA 116(29): 14414-14423.

PEZZA AB, RASHID HA & SIMMONDS I. 2012. Climate links and recent extremes in Antarctic sea ice, high-latitude cyclones, Southern Annular Mode and ENSO. Clim Dyn 38: 57-73.

RABELO LB, CRAUSS M & DE SOUZA RB. 2009. Estrutura Termal da Frente Polar na região da Passagem de Drake através de perfis verticais de temperatura obtidos com XBT. Cienc Nat 31: 313-316.

RAPHAEL MN. 2003. Impact of observed sea-ice concentration on the Southern Hemisphere extratropical atmospheric circulation in summer. J Geophys Res 108(D22): 4687.

RAPHAEL MN, HOBBS W & WAINER I. 2011. The effect of Antarctic sea ice on the Southern Hemisphere atmosphere during the southern summer. Clim Dyn 36: 1403-1417.

RAYNER NA, PARKER DE, HORTON EB, FOLLAND CK, ALEXANDER LV, ROWELL DP, KENT EC & KAPLAN A. 2003. Global analyses of sea surface temperature, sea ice, and night marine air temperature since the late nineteenth century. J Geophys Res 108(D14): 4407.

REICHLER T & KIM J. 2008. How Well Do Coupled Models Simulate Today's Climate? Amer Meteor Soc 89(3): 303-311.

RUDEVA I & SIMMONDS I. 2015. Variability and Trends of Global Atmospheric Frontal Activity and Links with Large-Scale Modes of Variability. J Clim 28(8): 3311-3330.

SCREEN JA, BRACEGIRDLE TJ & SIMMONDS I. 2018. Polar Climate Change as Manifest in Atmospheric Circulation. Curr Clim Change Rep 4: 383-395.

SEMTNER AJ. 1976. A Model for the Thermodynamic Growth of Sea Ice in Numerical Investigations of Climate. J Phys Oceanogr 6(3): 379-389.

SMITH DM, DUNSTONE NJ, SCAIFE AA, FIEDLER EK, COPSEY D & HARDIMAN SC. 2017. Atmospheric Response to Arctic and Antarctic Sea Ice: The Importance of Ocean–Atmosphere Coupling and the Background State. J Clim 30(12): 4547-4565.

SON SW, KIM SY & MIN SK. 2018. Widening of the Hadley Cell from Last Glacial Maximum to Future Climate. J Clim 31 (1): 267-281.

STOUFFER RJ ET AL. 2006. GFDL's CM2 Global Coupled Climate Models. Part IV: Idealized Climate Response. J Clim 19(5): 723-740.

SUN X, COOK KH & VIZY EK. 2017. The South Atlantic subtropical high: Climatology and interannual variability. J Clim 30(9): 3279-3296.

TAYLOR K, WILLIAMSON D & ZWIERS F. 2000. The Sea Surface Temperature and Sea-ice Concentration Boundary Conditions for AMIP II Simulations. Program for Climate Model Diagnosis and Intercomparison (PCMDI), p. 28.

THOMPSON DWJ & WALLACE JM. 2000. Annular modes in the extratropical circulation. Part I: Month-to-month variability. J Clim 13(5): 1000-1016.

TURNER J, GUARINO MV, ARNATT J, JENA B, MARSHALL GJ & PHILLIPS T. 2020. Recent decrease of summer sea ice in the Weddell Sea, Antarctica. Geophys Res Lett 47: e2020GL087127.

WANG Z, TURNER J, WU Y & LIU C. 2019. Rapid Decline of Total Antarctic Sea Ice Extent during 2014–16 Controlled by Wind-Driven Sea Ice Drift. J Clim 32(17): 5381-5395.

WINTON M. 2000. A Reformulated Three-Layer Sea Ice Model. J Atmos Oceanic Technol 17(4): 525-531.

WITTENBERG AT, ROSATI A, LAU NC & PLOSHAY JJ. 2006. GFDL'S CM2 Global Coupled Climate Models. Part III: Tropical Pacific Climate and ENSO. J Clim 19(5): 698-722.

YUAN X. 2004. ENSO-Related Impacts on Antarctic Sea Ice: A Synthesis of Phenomenon and Mechanisms. Antarct Sci 16(4): 415-425.

YUAN X, KAPLAN MR & CANE MA. 2018. The Interconnected Global Climate System - A Review of Tropical-Polar Teleconnections. J Clim 31(15): 5765-5792.

YUAN X & LI C. 2008. Climate Modes in Southern High Latitudes and Their Impacts on Antarctic Sea Ice. J Geophys Res Oceans 113(C6): C06S91.

YUAN X & MARTINSON DG. 2000. Antarctic Sea Ice Extent Variability and Its Global Connectivity. J Clim 13(10): 1697-1717.

YUAN X & MARTINSON DG. 2001. The Antarctic Dipole and its Predictability. Geophys Res Lett 28(18): 3609-3612.

SUPPLEMENTARY MATERIAL

Figures S1 – S3

How to cite

QUEIROZ MGS, PARISE CK, PEZZI LP, CARPENEDO CB, VASCONCELLOS FC, TORRES ALR, BARBOSA WL & LIMA LG. 2022. Response of southern troposphere meridional circulation to historical maxima of Antarctic sea ice. An Acad Bras Cienc 94: e20210795. DOI 10.1590/0001-3765202220210795.

Manuscript received on May 27, 2021;
accepted for publication on November 7, 2021

MICHELLY G.S. QUEIROZ[1]
https://orcid.org/0000-0002-4732-7911

CLÁUDIA K. PARISE[1]
https://orcid.org/0000-0002-9466-788X

LUCIANO P. PEZZI[2]
https://orcid.org/0000-0001-6016-4320

CAMILA B. CARPENEDO[3]
https://orcid.org/0000-0001-9034-789X

FERNANDA C. VASCONCELLOS[4]
https://orcid.org/0000-0002-5931-1503

ANA LAURA R. TORRES[1]
https://orcid.org/0000-0003-0155-4059

WESLEY L. BARBOSA[1]
https://orcid.org/0000-0002-9279-5626

LEONARDO G. LIMA[5]
https://orcid.org/0000-0001-7449-8639

[1]Universidade Federal do Maranhão (UFMA), Departamento de Oceanografia e Limnologia (DEOLI), Laboratório de Estudo e Modelagem Climática (LACLIMA), Avenida dos Portugueses, 1966, Vila Bacanga, 65080-805 São Luís, MA, Brazil

[2]Instituto Nacional de Pesquisas Espaciais (INPE), Laboratório de Estudos do Oceano e da Atmosfera (LOA), Divisão de Observação da Terra e Geoinformática (DIOTG), Avenida dos Astronautas, 1758, Jardim da Granja, 12227-010 São José dos Campos, SP, Brazil

[3]Universidade Federal do Paraná (UFPR), Departamento de Solos e Engenharia Agrícola (DSEA), Rua dos Funcionários, 1540, Cabral, 80035-050 Curitiba, PR, Brazil

[4]Universidade Federal do Rio de Janeiro (UFRJ), Departamento de Meteorologia, Avenida Athos da Silveira Ramos, 274, Cidade Universitária, 21941-916 Rio de Janeiro, RJ, Brazil

[5]Universidade Federal do Maranhão (UFMA), Departamento de Oceanografia e Limnologia (DEOLI), Laboratório de Estudos de Oceanografia Geológica (LEOG), Avenida dos Portugueses, 1966, Vila Bacanga, 65080-805 São Luís, MA, Brazil

Correspondence to: **Cláudia Klose Parise**
E-mail: claudiakparise@gmail.com

Author contributions

Michelly G.S. Queiroz processed the climate data, applied the methods and analyses and wrote the manuscript. Cláudia K. Parise performed the conceptualization of the manuscript, provided the numerical climate data, helped writing the manuscript, supervised the work. Ana Laura R. Torres and Wesley L. Barbosa were involved in the methodology. Luciano P. Pezzi has contributed with the infrastructure needed for carrying out the numerical experiments and helped to write the manuscript. Camila B. Carpenedo and Fernanda C. Vasconcellos performed the review and helped to discuss the results. Leonardo G. Lima helped with the creation and consolidation of the Laboratory for Climate Studies and Modelling (Laboratório de Estudo e Modelagem Climática - LACLIMA) at the Department of Limnology and Oceanography (Departamento de Oceanografia e Limnologia - DEOLI) in the Federal University of Maranhão (Universidade Federal do Maranhão - UFMA) where most analyses could be conducted.